

## Evaluation of Fracture Toughness of Pressure Vessel Steel Using Charpy Impact Test Specimens

Dae-June Han and Sun-Pil Choi  
Korea Advanced Energy Research Institute  
(Received February 3, 1987)

### Charpy 충격시편을 이용한 압력용기 재료의 파괴인성 측정

한 대 준 · 최 순 필

한국에너지연구소  
(1987. 2. 3 접수)

#### Abstract

The fracture toughness of SA 533 Grade B Class 1 steel has been studied with the Charpy impact test specimens in a range of temperature between  $-40^{\circ}\text{C}$  and  $288^{\circ}\text{C}$ . The dynamic fracture toughness is measured by the instrumented precracked Charpy impact test while the static fracture toughness is by the 3-point bend test based on the unloading compliance method. The results are compared with the data obtained from the large specimens.

It is known through the studies that temperature dependence of the appropriate (a low bound) value of the fracture toughness can be estimated by taking the static fracture toughness above the transition temperature and the dynamic fracture toughness below the temperature and it is also shown that the tests are satisfied with the requirements of ASTM E 813 when the side-groove is more than 14%.

#### 요 약

원자로 압력용기 재료인 SA 533 Grade B Class 1강의 파괴인성에 대하여  $-40^{\circ}\text{C} \sim 288^{\circ}\text{C}$ 의 온도 구간에서 Charpy 충격시편을 이용하여 연구하였다. 동적 파괴인성은 계장화 충격시험으로, 정적 파괴인성은 unloading compliance 방법에 따라 3-point bend test로 수행되었으며, 결과는 큰 시편에 의한 자료와 비교하였다.

온도에 대한 재료의 적절한 파괴인성치(하한값)는 천이온도 이상에서는 정적 파괴인성을, 그 이하의 온도에서는 동적 파괴인성을 택함으로써 유추할 수 있음을 알게 되었으며 side-groove가 14% 이상일 때 시험은 ASTM E 813의 조건을 만족함을 보였다.

#### Nomenclature

$a$  = crack length  
 $a_i$  = initial crack length

$a_f$  = final crack length  
 $b$  = Uncracked ligament length  
 $B$  = Specimen thickness  
 $C_m$  = Machine compliance  
 $C_s$  = Specimen compliance

- $Ct$  = Total compliance  
 $\delta L$  = Load line displacement  
 $\delta s$  = Specimen displacement  
 $E$  = Young's modulus  
 $\bar{E}m$  = Energy absorbed by deformation of the specimen up to crack extension  
 $E_m$  = Energy used in the test  
 $E_a$  = Energy calculated from area under load-time trace  
 $E_o$  = Total energy available in test  
 $J$  = J-integral (Ref. 4)  
 $P$  = Load  
 $P_{gy}$  = Load corresponding to general yielding  
 $P_m$  = Value of the load corresponding to crack extension  
 $r$  = Rotational factor =  $\begin{cases} 0.40(a/w < 0.49) \\ 0.45(a/w > 0.49) \end{cases}$   
 $T_{gy}$  = Time corresponding to general yielding  
 $V_g$  = Knife edge crack opening displacement  
 $V_o$  = Linear velocity of the striking point immediately before impact  
 $z$  = Knife edge thickness

## 1. Introduction

Exposure of nuclear reactor pressure vessels to neutron irradiation results in changes in mechanical properties as well as many other physical properties due to the production of atomic defects by high energy neutrons. These defects produce the phenomena, so-called radiation effects. The radiation embrittlement is a radiation effect on mechanical properties, that the hardness and the yield strength are increased while the ductility and the toughness are decreased, which increase the risk of brittle fracture of the reactor vessels.

The quantities assessing such effects are the changes in the nil-ductility transition temperature (RTndt) and the Charpy impact upper shelf energy (USE) measured regularly with surveillance specimens withdrawn from the reactor

during its life time. For the commercial reactors, ASTM E 185<sup>(1)</sup> describes the standard procedure for the surveillance test of the PWR type reactors. Among the mechanical tests, the Charpy impact test, the tensile test, and the fracture toughness test are evaluated with respect to the neutron fluence. So far the fracture toughness test is supplemental. However, when the materials do not satisfy the U.S. 10 CFR 50, App. G requirements<sup>(2)</sup> (RTndt at 1/4T exceeds 200°F or USE at 1/4T drops below 50 ft-lb), the fracture toughness is only the material property for analyzing the integrity of the pressure vessels. Therefore, it is necessary to evaluate the effects of irradiation on the fracture toughness of the component materials and to be able to estimate an appropriate value (a lower bound value) of the toughness at a specific time.

Generally, ASTM E 399<sup>(3)</sup> and ASTM E 813<sup>(4)</sup> are applied to evaluate the fracture toughness. And the E 813 has some advantages since it uses the unloading compliance method with a single specimen and relatively small size specimen compared with the E 399. However the number and the size of the fracture toughness specimens are very limited as shown in Table I because of a limited space in the commercial reactors. On the other hand, the number of the Charpy specimens is about 15 for each material and only seven or eight specimens are needed for a full curve of the Charpy test. Therefore, if it is possible to use the Charpy specimens for the fracture toughness, the rest of the specimens can be used for the additional informations on the fracture toughness and for assuring the fracture behaviour of the materials.

In the present studies, the static and the dynamic fracture toughness are measured with the Charpy specimens by the slow bend and by the instrumented impact machine, respectively

**Table I. Quantities of Mechanical Property Test Specimens in One Surveillance Capsules of Some Commercial Reactors.**

		Charpy	Tension	Fracture Toughness
KO-RI Unit 1	Base Metal { Tangential	12	3	3*
	{ Axial	12	3	3
	Weld Metal	12	3	3
	HAZ	12	—	—
KO-RI Unit 2	Base Metal { Longitudinal	15	3	4**
	{ Transverse	15	3	4
	Weld Metal	15	3	4
	HAZ	15	—	—
KO-RI Unit 5	Base Metal { Longitudinal	15	3	4**
	{ Transverse	15	3	4
	Weld Metal	15	3	4
	HAZ	15	—	—

\* 1T WOL Specimen    \*\* 1/2T C/T Specimen

and compared with the data from large size specimens in the literatures in order to make a correlation for a lower bound value of the fracture toughness.

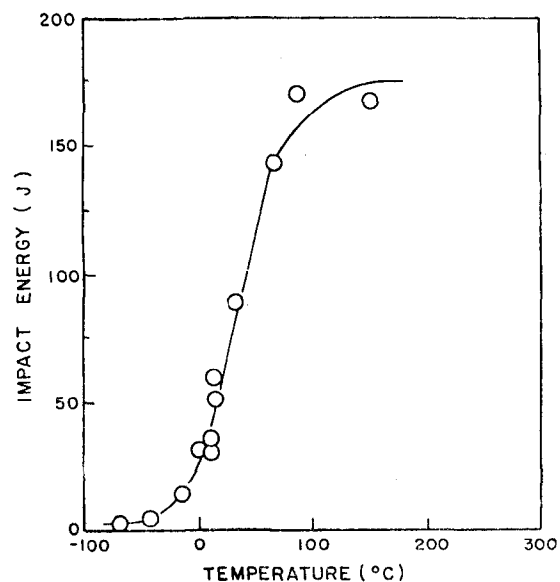
## 2. Experiments

### 2.1. Material

The materials for the studies is SA 533 Grade B Class 1 plate, the well known nuclear reactor pressure vessel material.<sup>(5)</sup> The tensile properties are given in Table II and the impact energy is shown in Fig. 1. The temperatures for the fracture toughness test are determined based on the impact test results. They are  $-40^{\circ}\text{C}$  which is below the NDT and at which the fracture toughness test results of 1T C/T specimens are available;  $35^{\circ}\text{C}$ , the transition region,  $90^{\circ}\text{C}$ , the temperature at the upper knee; and  $288^{\circ}\text{C}$  which is the operating temperature.

**Table II. Tensile Properties of SA 533 Grade B Class 1 Steel.**

Yield Strength (MPa)	Ultimate Tensile Strength (MPa)	Elongation (%)	Reduction of Area (%)
490.8	685.4	20.7	61.7

**Fig. 1. Charpy Impact Test Results of SA 533 Grade B Class 1 Steel.**

All specimens for impact test are the standard Charpy impact specimens machined according to the method of ASTM E 23, and fatigue-cracked to about  $a/w=0.55$ .<sup>(4)</sup> Some of the specimens are side-grooved to 14% and 25% following the fact that the Charpy specimens with side-groove more than 12% of the specimen thickness could give same static results as 1T C/T specimens.<sup>(6)</sup> Kinds

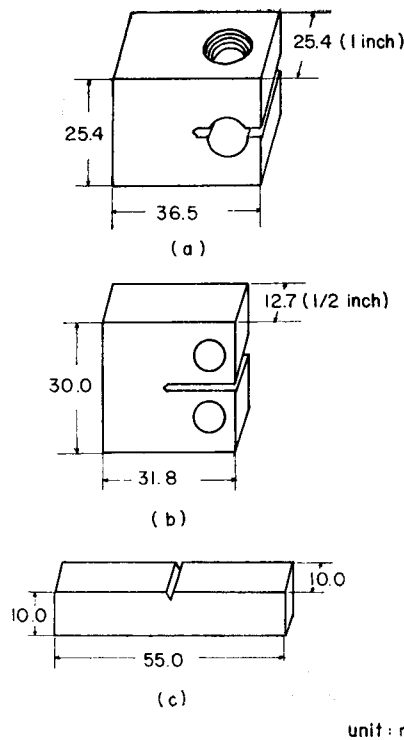


Fig. 2. Fracture Toughness Test Specimens. (a) 1 T WOL Specimen, (b) ASTM E-399 Type 1/2T C/T Specimen, (c) ASTM E-23 Type Charpy Impact Test Specimen.

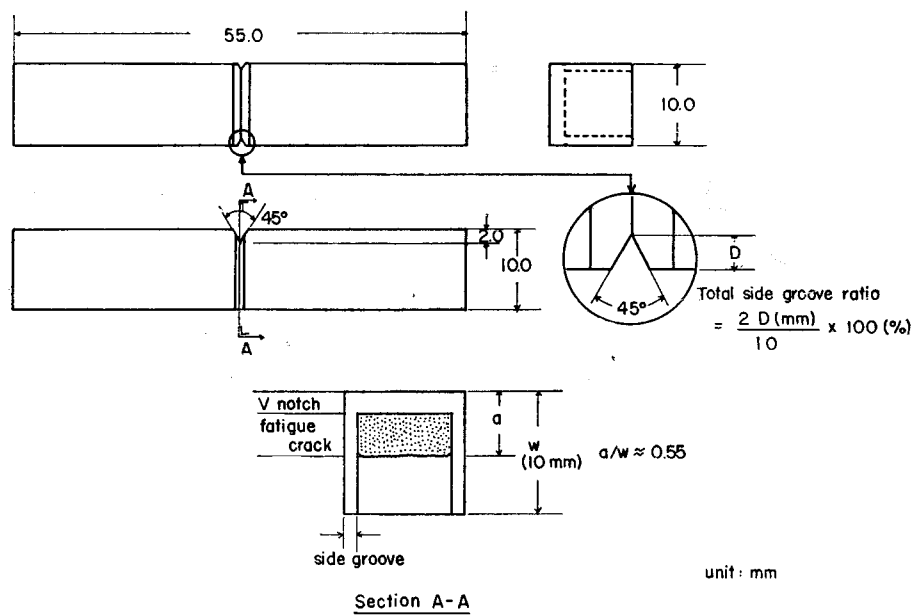


Fig. 3. Schematic Diagrams of the Precracked Charpy Impact Test Specimen Tested in This Experiment.

of fracture toughness test specimens are shown in Fig. 2, and the schematic diagram of the Charpy impact test specimen tested in this experiment is shown in Fig. 3.

## 2.2 Dynamic Fracture Toughness Test

The dynamic fracture toughness is measured by the instrumented Charpy impact tester which consists of a Baldwin impact tester, Dynatup 500 instrument system, Nicolet storage oscilloscope, and HP 9825B computer which accumulate the data signals and calculate the J values and the fracture toughness. The circuit diagram and the flow chart of the test are shown in Fig. 4 and Fig. 5.

The specimen temperature is controlled by the electrical heating of carbon electrode in high temperatures and by liquid nitrogen below the room temperature.

$J_{Id}$  is calculated by the following equations<sup>(7)</sup>;

$$J_{Id} = 2 \cdot \bar{E}m / bB$$

where

$$\bar{E}m = Em - 1/2 Pm^2 \cdot Cm^2$$

$$Em = Ea(1 - Ea/4Eo)$$

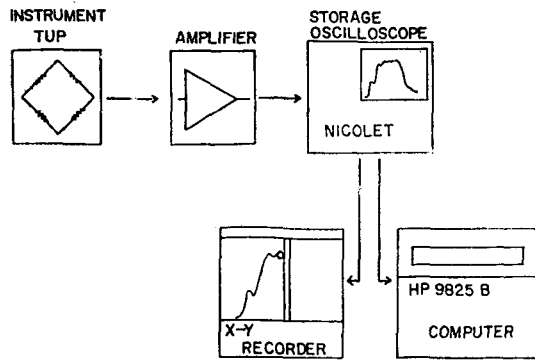


Fig. 4. Circuit Diagrams of the Instrumented Precracked Charpy Impact Test.

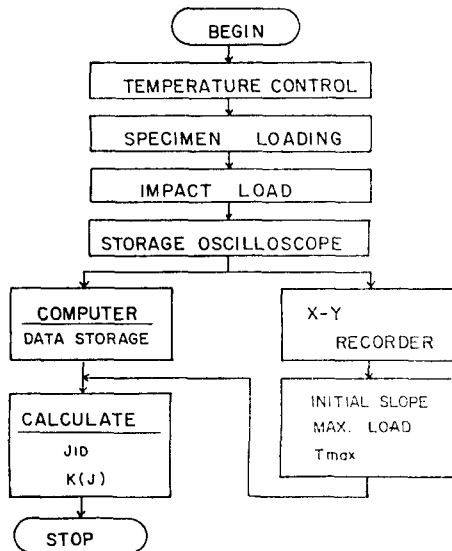


Fig. 5. Flow Chart of the Instrumented Precracked Charpy Impact Test.

$$\begin{aligned}
 C_m &= C_t - C_s \\
 C_t &= V_o \cdot T_{gy} / P_{gy} \\
 C_s &= \delta s / P = C_s^* / EB \\
 C_s^* &= 72f(a/w) + 20 \\
 f(a/w) &= 1.8625(a/w)^2 - 3.95(a/w)^3 \\
 &\quad + 16.3777(a/w)^4 - 37.2277(a/w)^5 \\
 &\quad + 77.554(a/w)^6 - 126.873(a/w)^7 \\
 &\quad + 175.533(a/w)^8 - 143.964(a/w)^9 \\
 &\quad + 66.564(a/w)^{10}
 \end{aligned} \quad (8)$$

and all quantities, not given by the above relations, are obtained from the load-displacement

curve.

$K_{Id}$  is then obtained from  $J_{Id}$  through the equation;

$$K_{Id} = (E \cdot J_{Id})^{1/2} = K(J)$$

It is difficult to calculate fracture toughness directly from the raw load signal since the signal is superimposed with the real load signal and a sinusoidal noise, resulting in a serrated oscillation. To reduce such an oscillation, the initial energy is adjusted to a value between 25 and 264 ft-lb. And when the oscillation becomes too large to be adjusted, the moving average method<sup>(9)</sup> should be used.

### 2.3. Static Fracture Toughness Test

3-point bend test is carried out with a dynamic MTS of 10 ton capacity and HP 9836 computer which are connected to an interface and A/D converter, so that the computer can control the MTS. The testing apparatus is shown in Fig. 6. And the circuit diagram and the flow chart of the experimental processes are shown in Fig. 7 and Fig. 8.

The modified J suggested by Ernst<sup>(10)</sup> and the unloading compliance method are applied for evaluation of the fracture toughness. The equation for calculating the compliance is very important in the unloading compliance method

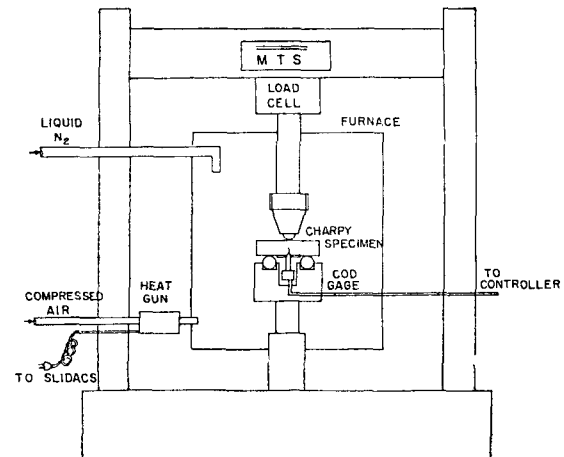


Fig. 6. Schematic Diagrams of Testing Apparatus for the 3-Point Bend Test.

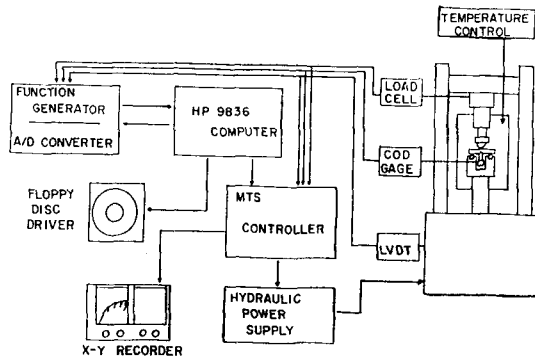


Fig. 7. Circuit Diagrams of the 3-Point Bend Test.

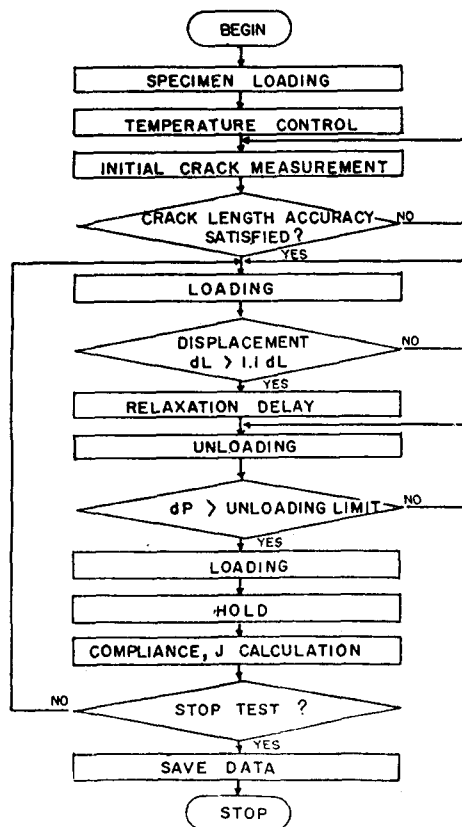


Fig. 8. Flow Chart of the 3-Point Bend Test.

because the output signal from the C.O.D. gage is converted to a crack length through that equation. For such an equation, we are going to take Nanstad's relation<sup>(11)</sup>, which is

$$EB\delta L/P = -307.956 + 4573.694(a/w) - 24214.57(a/w)^2 + 61685.2(a/w)^3 - 75188.3(a/w)^4 + 35860.5(a/w)^5$$

However the above equation is not in a good shape since it is the compliance as a function of the crack length. Therefore an equation for the crack length should be deduced as a function of the compliance.

$$\text{If } Ux = \{(EB\delta L/P) + 1\}^{-1/2},$$

then Nanstad's relation can be modified as follows approximately

$$a/w = 1.038 - 8.0Ux + 117.3(Ux)^2 - 1488.2(Ux)^3 + 8398.2(Ux)^4 - 17921.5(Ux)^5$$

In actual tests, the compliances are measured. With the known conditions of the specimen, the compliance is converted to the loadline compliance through the equation;

$$EB\delta L/P = EB\delta Vg/P \times w/(z + a + rb)$$

With the loadline compliance,  $Ux$  and  $a/w$  are calculated. After several iterations,  $a/w$  converges to a value within a certain accuracy, the calculated  $a/w$  is compared with the measured crack length after test, and is in good agreement with the present experimental results.

$J_{1C}$  and  $K_{1C}$  are calculated following the ASTM E 813 method.

### 3. Results

#### 3.1. Instrumented Impact Test

The absorbed energy (dial energy, energy shown on the dial of the tester) is measured with pre-cracked Charpy specimens with respect to the temperatures and is shown in Fig. 9. Comparing Fig. 9 with Fig. 1, which is the absorbed energy measured with un-cracked specimens, the value of the former is reduced by a factor of about four, while the shape of the full curve is almost unchanged. The reasons for the reduction may be due to the reduced cross sectional area by the fatigue crack and the accute crack front, so that the cracked specimen would be broken much more easily.

Fig. 10 is an auxiliary figure to show that

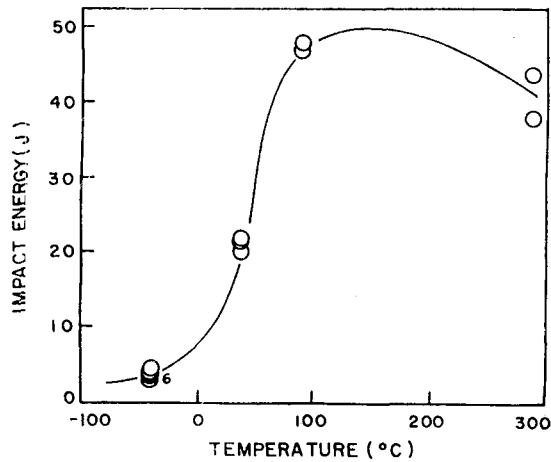


Fig. 9. Charpy Impact Test Results of the Instrumented Precracked Charpy Impact Test.

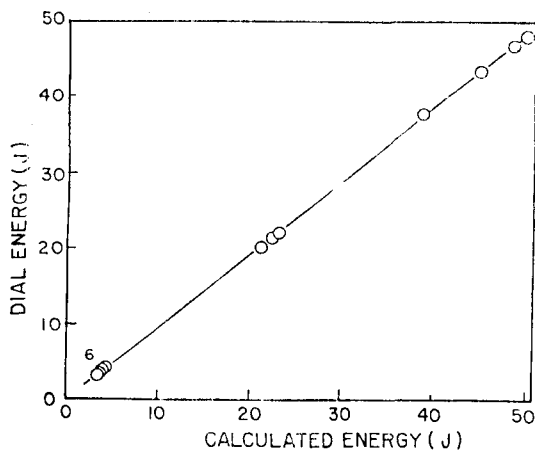


Fig. 10. Relationship between the Dial Energy and the Energy Calculated from the Load-time Trace of The Instrumented Precracked Charpy Impact Test.

the test machine is calibrated well. The energy as the area under the load-time (displacement) trace is plotted with respect to the dial energy, showing a linear relationship.

The values of  $K_{Id}$  ( $K(J)$ ) from the instrumented impact test are plotted in Fig. 11, from which a value of  $K_{Id}$  in the upper shelf region is obtained to be about  $260 \text{ MPa m}^{1/2}$ .

### 3.2. 3-Point Bend Test

After the tests, the specimens are broken and the actual crack lengths, both the initial crack

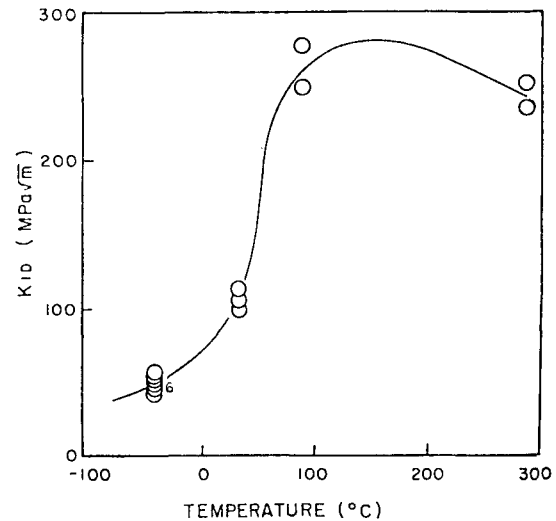


Fig. 11. Variations of the Dynamic Fracture Toughness:  $K_{Id}$  from the Instrumented Precracked Charpy Impact Test with Temperature.

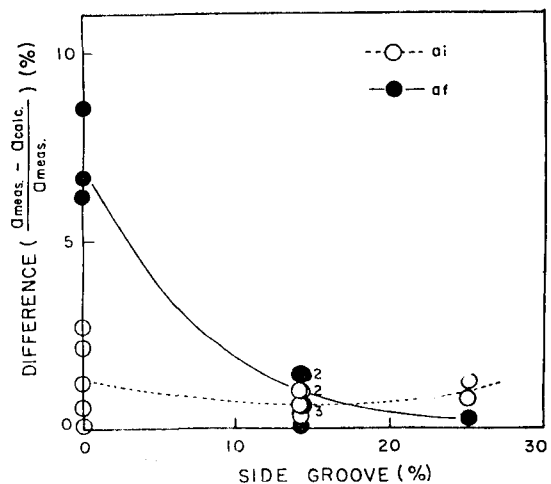


Fig. 12. Difference between the Measured Crack Length and the Calculated Crack Length with side Grooves.

length and crack extension, are measured according to the standard method. The differences between the measured crack length and the crack length calculated by the unloading compliance method are plotted in Fig. 12 for the initial and the final crack length and in Fig. 13 for the crack extensions. The differences for the initial crack lengths are less than 3%

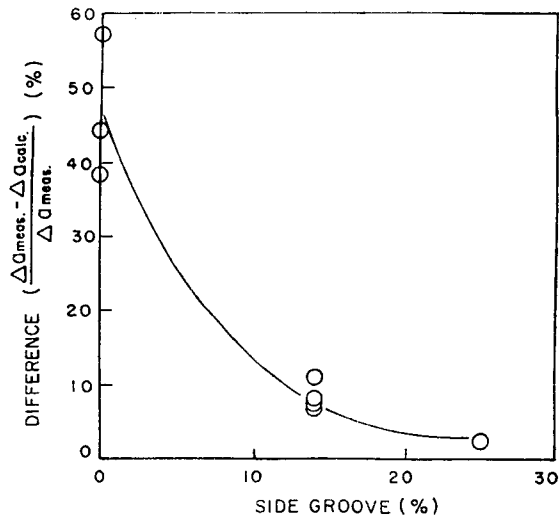


Fig. 13. Difference between the Measured Crack Growth and the Calculated Crack Growth during the Test with Side Grooves.

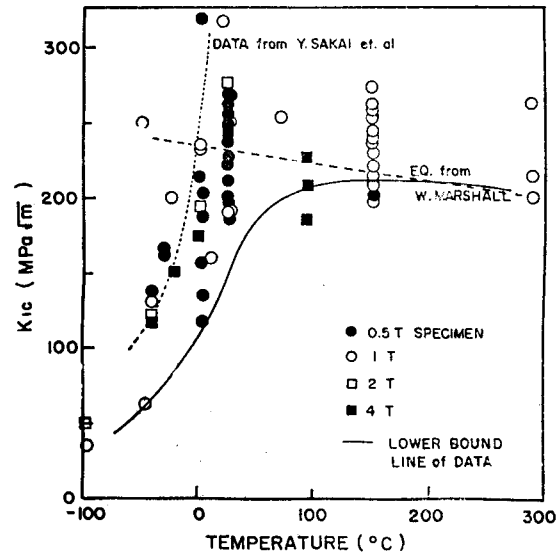


Fig. 15. Fracture Toughness Data for the SA 533 Grade B Class 1 Steel from some References.

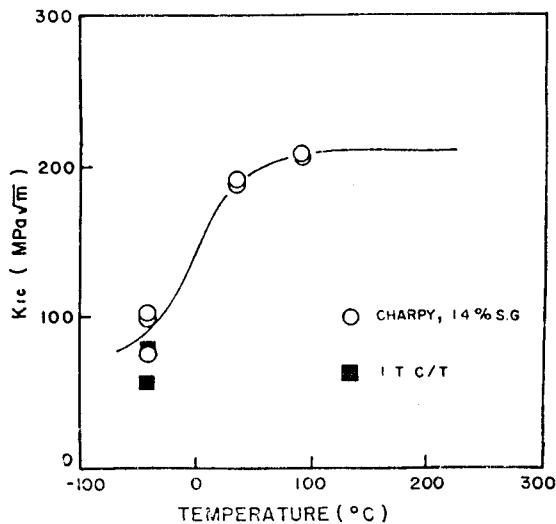


Fig. 14. Variations of the Static Fracture Toughness:  $K_{Ic}$  from the 3-Point Bend Test with Temperature.

regardless of the side groove depths, while those for the final crack lengths and crack extension decrease as the side groove depths increases. And it is shown that when the side groove depth is more than 14% the difference comes down below 12% which is the requirement of ASTM E 813.

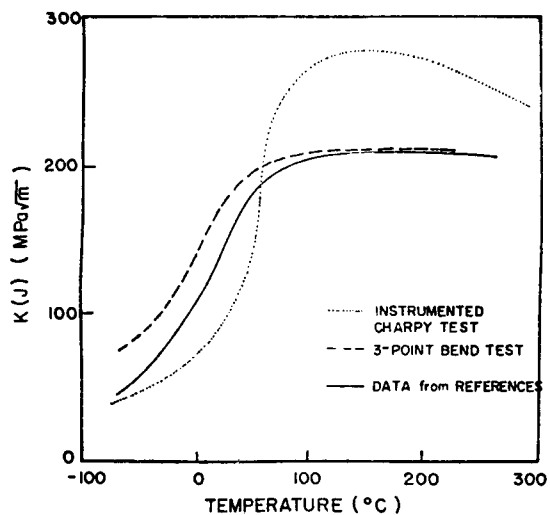


Fig. 16. Comparisons of Dynamic and Static Fracture Toughness Test Results.

The values of  $K_{Ic}$  respect to the temperatures are shown in Fig. 14, from which  $K_{Ic}$  in the upper shelf region is obtained to be about 200  $MPa m^{1/2}$ , which agrees well with the results obtained from 1T C/T specimen at  $-40^{\circ}C$ .

### 3.3. Evaluation of the Results

Fig. 15 is a collection of the fracture toughness data of SA533 Grade B Class 1 steel tested



with HSST 02\* and HSST 03\* Plate and the solid line represents the lower bound values of the fracture toughness of the steel. The present experimental results are compared with the lower bound values in Fig. 16, showing that the dynamic fracture toughness is close to the lower bound value below the transition region while the static fracture toughness is close to the lower bound value above the transition region. Therefore if we perform the fracture toughness test with the pre-cracked Charpy specimens and take the values in such a way, then we are going to have a good and simple method to estimate the lower bound values of the fracture toughness of the materials.

#### 4. Conclusion

It is concluded for the fracture toughness of SA 533 Grade B Class 1 steel, the nuclear pressure vessel material, that

1. The initial crack length and the crack extension can be estimated by the unloading compliance method within uncertainty of 3% and 12%, respectively, when the side groove depth is more than 14%.
2. The lower bound values of the fracture toughness can be taken as the dynamic fracture toughness below the transition region and the static fracture toughness above the transition region for conservatism.

#### References

1. "Standard Practice for Conducting Surveillance Tests for Light-Water Cooled Nuclear Power Reactor Vessels", ASTM E 185-82, ASTM
2. 10CFR50 50-55 a, Appendix G, 1983 Revision
3. "Standard Test Method for Plane-Strain Fracture Toughness of Metallic Materials", ASTM E399-83, ASTM
4. "Standard Test Method for  $J_{1c}$ , A Measure of Fracture Toughness", ASTM E 813-81, ASTM
5. W.R. Corwin, G.C. Robinson, R.K. Nanstad, J.G. Merkle, R.G. Berggren, G.M. Goodwin, R.L. Swain and T.D. Owings, "Effects of Stainless Steel Weld Overlay Cladding on the Structural Integrity of Flawed Steel Plates in Bending", NUREG/CR-4015, ORNL/TM-9390 (1985)
6. W.L. Server, J.M. Sheckherd and R.A. Wullaert, "Novel Techniques for Determining Upper Shelf Dynamic Initiation Toughness in Nuclear Pressure Vessel Steels", CSNI Specialist Meeting on Instrumented Precracked Charpy Testing, EPRI NP-2102-LD (1981) pp. 4-39-4-58.
7. "Instrumented Precracked Charpy Testing for Medium Strength Nuclear Pressure Vessel Steels", PVRC/MPC Task Group on Fracture Toughness Properties for Nuclear Components, Welding Research Council (1977)
8. W.L. Server, D.R. Ireland and R.A. Wullaert, "Strength and Toughness Evaluation from an Instrumented Impact Test", ETI Report TR 74-29R (1974)
9. T. Kobayashi, "Analysis of Impact Properties of A533 Steel for Nuclear Reactor Pressure Vessel by Instrumented Charpy Test", Engineering Fracture Mechanics, Vol. 19, No. 1, (1984) pp. 49-65.
10. H.A. Ernst, "Material Resistance and Instability beyond J-Controlled Crack Growth", ASTM STP 803 (1983) pp. I-191-I-213.
11. R.K. Nanstad, Unpublished Data

\* HSST Plate: Heavy section pressure vessel steel plate produced for the HSST (Heavy Section Steel Technology) project. HSST 02 and 03 plates are SA 533 B 1, and the numbers following HSST are identification numbers of the specimens.